COMPUTER METHODS AND PROGRAMS IN BIOMEDICINE 108 (2012) 80–89

journal homepage: www.intl.elsevierhealth.com/journals/cmpb

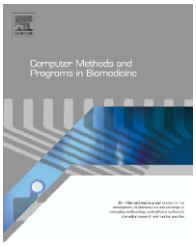

Efficient inhomogeneity compensation using fuzzy c-means clustering models

László Szilágyi[a,b], Sándor M. Szilágyi[a,b,*], Balázs Benyó[b]

[a] Sapientia University of Transylvania, Faculty of Technical and Human Sciences, Şoseaua Sighişoarei 1/C, 540485 Tîrgu Mureş, Romania[1]

[b] Budapest University of Technology and Economics, Department of Control Engineering and Information Technology, Magyar tudósok krt. 2, H-1117 Budapest, Hungary[2]

ARTICLE INFO

Article history:
Received 25 October 2011
Received in revised form
28 December 2011
Accepted 14 January 2012

Keywords:
Image segmentation
Magnetic resonance imaging
Intensity inhomogeneity
c-Means clustering
Histogram

ABSTRACT

Intensity inhomogeneity or intensity non-uniformity (INU) is an undesired phenomenon that represents the main obstacle for magnetic resonance (MR) image segmentation and registration methods. Various techniques have been proposed to eliminate or compensate the INU, most of which are embedded into classification or clustering algorithms, they generally have difficulties when INU reaches high amplitudes and usually suffer from high computational load. This study reformulates the design of c-means clustering based INU compensation techniques by identifying and separating those globally working computationally costly operations that can be applied to gray intensity levels instead of individual pixels. The theoretical assumptions are demonstrated using the fuzzy c-means algorithm, but the proposed modification is compatible with a various range of c-means clustering based INU compensation and MR image segmentation algorithms. Experiments carried out using synthetic phantoms and real MR images indicate that the proposed approach produces practically the same segmentation accuracy as the conventional formulation, but 20–30 times faster.

1. Introduction

Magnetic resonance imaging (MRI) is a popular medical imaging modality due to its high resolution and good contrast. However, the automatic segmentation of such images is not trivial because of the noise that may be present. Intensity inhomogeneity or intensity non-uniformity (INU) represents an undesired phenomenon in MRI, manifested as a slowly varying bias field with possibly high magnitude that makes pixels belonging to the same tissue be observed with different intensities. Further on, INU is the main obstacle for intensity based segmentation methods: several efficient and accurate removal techniques exist for high frequency noise [6], but the segmentation in the presence of inhomogeneities is a process with significant computational load [26].

Inhomogeneities in magnetic resonance (MR) images are usually categorized by their origin. Device related INU artifacts can be efficiently compensated via calibration methods based on prior information obtained by using a uniform phantom [2]. Alternately, INU artifacts related to the shape, position, structure and orientation of the patient [15], are much more difficult to handle [26]. Several retrospective INU compensation approaches have been reported, which include

* *Corresponding author at*: Sapientia University of Transylvania, Faculty of Technical and Human Sciences, Şoseaua Sighişoarei 1/C, 540485 Tîrgu Mureş, Romania.

E-mail addresses: lalo@ms.sapientia.ro (L. Szilágyi), szs@ms.sapientia.ro (S.M. Szilágyi), bbenyo@iit.bme.hu (B. Benyó).

0169-2607/$ – see front matter © 2012 Elsevier Ireland Ltd. All rights reserved.
doi:10.1016/j.cmpb.2012.01.005

homomorphic filtering [5,9], polynomial or B-spline surface fitting based on intensity [23] or gradient [24], segmentation based techniques via maximum likelihood estimation [14], Markov random fields [27], fuzzy c-means clustering [4,13,16], or nonparametric estimation [7]. Further INU compensation procedures based on histogram involve high-frequency maximization [17], information maximization [25], or histogram matching [18]. The most complete review of INU compensation techniques can be found in [26].

Probably the most widely used compensation tool is the fuzzy c-means (FCM) algorithm [3], having several adaptations for INU estimation and being combined with a series of further techniques. In this order, Pham and Prince introduced a modified objective function producing bias field estimation and containing extra terms that force this artifact vary smoothly [13]. They also provided a multi-grid technique to speed up the computationally heavy algorithm, but even this way, their algorithm performs slowly. Liew and Hong created a log bias field estimation technique that models the INU with smoothing B-spline surfaces [11]. Ahmed et al. established a regularization operator that allowed the labeling of a pixel to be influenced by its immediate neighbors [1]. This approach reduced some of the complexity of its ancestors, but the zero gradient condition that was used for bias field estimation leads to several misclassifications. Siyal and Yu [16] provided a mean spread filtering method to smoothen the estimated bias field in every cycle of the FCM algorithm, thus reducing the amount of necessary computations, but the result of the segmentation is not deterministic due to the nature of the smoothing filter. Szilágyi et al. [21] applied mixtures of fuzzy [3] and possibilistic [10] c-means clustering models, and showed their beneficial effects on the accuracy.

The compensation of INU artifacts is a computationally costly problem, which demands highly efficient design and implementation. This paper demonstrates that the INU compensation on a single-channel intensity image via c-means clustering models can be performed much more efficiently than it is reported in previous formulations. The operations performed during the iterations of the alternating optimization (AO) scheme are separated into globally working ones and locally applied ones, and their execution is optimized according to their necessities. Global criteria are applied to gray intensities instead of individual pixels, which makes a drastic reduction of the computational load. Using this novel formulation, and applying it to improved clustering models (e.g. [12,21]) combined with multi-stage INU compensation, can make c-means clustering more attractive on the combined scales of accuracy and efficiency. Improving the accuracy is not in the scope of this paper. Our main goal is to reduce the execution time without damaging the accuracy.

The rest of the paper is organized as follows. Section 2 describes the background works based on fuzzy c-means clustering. Section 3 presents the details on the proposed reformulation of the c-means clustering based INU compensation and segmentation method. Section 4 provides a qualitative and quantitative analysis and short discussion of segmentation results. In Section 5 the conclusions are formulated.

2. Background works

2.1. Conventional FCM clustering

The conventional FCM algorithm optimally partitions a set of object data into a previously set number of c clusters based on the iterative minimization of a quadratic objective function. When applied to segment gray-scale images, FCM clusters the intensity value of pixels x_k, $k = 1 \dots n$. The objective function

$$J_{FCM} = \sum_{i=1}^{c}\sum_{k=1}^{n} u_{ik}^{m}(x_k - v_i)^2, \tag{1}$$

is optimized under the so-called probability constraint

$$\sum_{i=1}^{c} u_{ik} = 1 \quad \forall\ k = 1 \dots n, \tag{2}$$

where $u_{ik} \in [0, 1]$ is the fuzzy membership function indicating the degree to which pixel k is assigned to cluster i, v_i represents the centroid or prototype of the ith cluster, and $m > 1$ is the fuzzy exponent or fuzzyfication parameter. The constrained optimization of the objective function is achieved using Lagrange multipliers and zero gradient conditions. The minimization of the cost function is reached by alternately applying the optimization of J_{FCM} over $\{u_{ik}\}$, $i = 1 \dots c$, $k = 1 \dots n$ with v_i fixed, and the optimization of J_{FCM} over $\{v_i\}$, $i = 1 \dots c$, with u_{ik} fixed [3]. In each cycle, optimal fuzzy membership and optimal cluster centroid values are computed using the formulas:

$$u_{ik} = \frac{(x_k - v_i)^{-2/(m-1)}}{\sum_{j=1}^{c}(x_k - v_j)^{-2/(m-1)}} \quad \forall\ i = 1 \dots c,\ \forall\ k = 1 \dots n, \tag{3}$$

and

$$v_i = \frac{\sum_{k=1}^{n} u_{ik}^{m} x_k}{\sum_{k=1}^{n} u_{ik}^{m}} \quad \forall\ i = 1 \dots c. \tag{4}$$

After adequate initialization of cluster prototype values v_i, Eqs. (3) and (4) are alternately applied until the norm of the variation of cluster prototypes stays within a previously set bound ε. This algorithm is called the AO scheme of FCM. Finally, each pixel k is assigned to the class w_k where

$$w_k = \arg\max_{i}\{u_{ik}, i = 1 \dots c\}. \tag{5}$$

2.2. INU compensation models

The FCM approach formulated so far clusters the set of data $\{x_k\}$, which was recorded among ideal circumstances, containing no noise. However, in the real case, the observed data $\{y_k\}$ differs from the actual one $\{x_k\}$. In this paper we only assume to handle the INU artifacts, by compensating during segmentation.

Literature recommends three different data variation models for intensity inhomogeneity. If we consider the INU as a bias field, for any pixel k, $k = 1 \dots n$ we will have

$$y_k = x_k + b_k, \tag{6}$$

where b_k represents the bias value at pixel k [1,13,16]. In case of gain field modeling [20], there will be a gain value g_k for each pixel k, such that

$$y_k = g_k x_k. \tag{7}$$

Finally, the so-called log bias approach in fact is a gain field estimation reduced to bias computation using the logarithmic formula [11]

$$\log y_k = \log g_k + \log x_k. \tag{8}$$

Regardless of the used compensation model, the variation of the intensity between neighbor pixels has to be slow. The zero gradient conditions derived from FCM's objective function does not fulfill this demand. Consequently, a smoothing operation is necessary to assure this slow variation of the estimated bias or gain field.

2.3. *Adaptation of FCM to bias field estimation*

Using the notions introduced above, in case of estimating the INU artifact as a bias field, the objective function becomes:

$$J_{\text{FCM-b}} = \sum_{i=1}^{c}\sum_{k=1}^{n} u_{ik}^{m}(y_k - b_k - v_i)^2. \tag{9}$$

Zero gradient conditions and Lagrange multipliers lead to the following optimization formulas:

- For any pixel with index $k = 1 \dots n$ and any cluster indexed $i = 1 \dots c$, the fuzzy partition is built of membership functions computed as:

$$u_{ik} = \frac{(y_k - b_k - v_i)^{-2/(m-1)}}{\sum_{j=1}^{c}(y_k - b_k - v_j)^{-2/(m-1)}}. \tag{10}$$

- For any cluster indexed $i = 1 \dots c$, we have:

$$v_i = \frac{\sum_{k=1}^{n} u_{ik}^{m}(y_k - b_k)}{\sum_{k=1}^{n} u_{ik}^{m}}. \tag{11}$$

- For any pixel with index $k = 1 \dots n$, we have the bias estimated as:

$$b_k = y_k - \frac{\sum_{i=1}^{c} u_{ik}^{m} v_i}{\sum_{i=1}^{c} u_{ik}^{m}}. \tag{12}$$

The whole AO algorithm of bias estimation and fuzzy c-means based segmentation is summarized in Table 1. This INU estimation and compensation approach was applied by Siyal and Yu [16].

Table 1 – The conventional algorithm.

01	$t = 0$
02	Set initial bias field $b_k^{(t=0)} = 0, \ \forall k = 1 \dots n$
03	Choose initial cluster prototypes $v_i^{(t=0)}$
04	Repeat
05	$t \leftarrow t + 1$
06	Compute new fuzzy partition $u_{ik}^{(t)}, \ \forall i = 1 \dots c$ and $\forall k = 1 \dots n$, using Eq. (10)
07	Compute new cluster prototypes $v_i^{(t)}, \ \forall i = 1 \dots c$, using Eq. (11)
08	Compute new estimated bias field $b_k^{(t)}, \ \forall k = 1 \dots n$, using Eq. (12)
09	Smoothen the estimated bias field using the chosen filter
10	Until convergence occurs, that is $\sum_{i=1}^{c} \lvert v_i^{(t)} - v_i^{(t-1)} \rvert < \varepsilon$
11	Assign pixel with index k ($k = 1 \dots n$) to cluster with index $\underset{i}{\arg\max}\{u_{ik}, i = 1 \dots c\}$

3. Methodology

When a clustering algorithm is required to perform quickly on a large set of input data, the aggregation of similar input values is an easily implementable choice. It is well known, that the FCM algorithm in image processing belongs to the segmentation methods that use only global information. This means that pixels will be assigned to clusters based on their own intensity (color), without regard to their position in the image. Consequently, pixels with same intensity will belong to the same clusters with the same membership degrees. Based on this assumption, it is obvious that the FCM-based segmentation of single-channel intensity image can be performed using the histogram, clustering the intensity levels instead of individual pixels. For further reading on quick, histogram based segmentation of brain MR images with homogeneous intensity, the reader is referred to [19].

On the other hand, when INU artifacts are present, local conditions need to be involved into the compensation process, because the level of the low-frequency noise that is present must be estimated for each pixel individually. The main loop of the AO algorithm of the conventional solution (FCM-b) contains three formulas to be evaluated, which all contain the locally estimated noise b_k. These computations treat each pixel separately, leading to a high computational load. Pixels that have similar intensities in the original image cannot be aggregated, as the locally present noise frequently makes them different.

In the following, we will demonstrate that the problem can be reformulated such a way, which allows us at the beginning of each loop, to aggregate the similar pixels in the current compensated image. This way we get the possibility to perform most part of the computations based on intensities, leading to a drastic reduction of the computational load.

3.1. *The accelerated approach*

Let us consider the cost function of the bias estimation approach, given in Eq. (9). The input image contains pixels in order of 10^4–10^5, and intensity levels in order of 10^2–10^3. In every iteration of the AO algorithm, we need to aggregate those

pixels, which bear the same intensity after having the current estimated bias subtracted. That is why, we investigate the distribution of the composite variable $y_k - b_k$, which varies from iteration to iteration. Let us denote by $h_l^{(t)}$ the number of pixels for which the compensated intensity in iteration t satisfies $y_k - b_k = l$. Obviously, if we denote by $\Omega^{(t)}$ the range of possible values of $y_k - b_k$, we will have $\sum_{l\in\Omega^{(t)}} h_l^{(t)} = n$. As the matter of fact, $h_l^{(t)}$ with $l \in \Omega^{(t)}$ represents the intensity histogram of the compensated image in iteration t.

Using the above notations, we can aggregate equal values of $y_k - b_k$ in the cost function without altering the sum, which in iteration t will become:

$$J_{\text{FCM-qb}} = \sum_{i=1}^{c}\sum_{l\in\Omega^{(t)}} h_l^{(t)} u_{il}^m (l - v_i)^2. \tag{13}$$

The update formulas for degrees of membership u_{il} and cluster prototypes v_i, $i = 1\dots c$, $l \in \Omega^{(t)}$ are obtained from the zero gradient conditions of the functional:

$$\mathcal{L}_{\text{FCM-qb}} = J_{\text{FCM-qb}} + \sum_{l\in\Omega^{(t)}} \lambda_l \sum_{i=1}^{c} \left(1 - \sum_{i=1}^{c} u_{il}\right), \tag{14}$$

where λ_l represent the Lagrange multipliers. From the partial derivatives with respect to u_{il}, for any $i = 1\dots c$, $l \in \Omega^{(t)}$ we obtain:

$$\frac{\partial \mathcal{L}_{\text{FCM-qb}}}{\partial u_{il}} = 0 \Leftrightarrow m u_{il}^{m-1} (l - v_i)^2 - \lambda_l = 0 \tag{15}$$

and consequently

$$u_{il} = \left[\frac{\lambda_l}{m}\right]^{-1/(m-1)} (l - v_i)^{-2/(m-1)}. \tag{16}$$

On the other hand, the probabilistic constraint given in Eq. (2) leads to:

$$\sum_{j=1}^{c} u_{jl} = 1 \Rightarrow 1 = \left[\frac{\lambda_l}{m}\right]^{-1/(m-1)} \sum_{j=1}^{c} (l - v_j)^{-2/(m-1)}. \tag{17}$$

Eqs. (16) and (17) imply that for any compensated intensity $l \in \Omega^{(t)}$ and any cluster indexed $i = 1\dots c$, we have the membership update formula:

$$u_{il} = \frac{(l - v_i)^{-2/(m-1)}}{\sum_{j=1}^{c} (l - v_j)^{-2/(m-1)}}, \tag{18}$$

One evaluation of the above formula computes the fuzzy labels of $h_l^{(t)}$ pixels at the same time. The obtained fuzzy membership values do not depend on the current histogram.

Zero crossing conditions of the partial derivatives with respect to cluster prototypes v_i lead to:

$$\frac{\partial \mathcal{L}_{\text{FCM-qb}}}{\partial v_i} = 0 \Leftrightarrow -2 \sum_{l\in\Omega^{(t)}} h_l^{(t)} u_{il}^m (l - v_i) = 0, \tag{19}$$

Table 2 – The proposed algorithm.

01	$t = 0$
02	Set initial bias field $b_k^{(t=0)} = 0,\ \forall k = 1\dots n$
03	Choose initial cluster prototypes $v_i^{(t=0)}$
04	Repeat
05	$t \leftarrow t + 1$
06	Compute new histogram $h_l^{(t)},\ \forall l \in \Omega^{(t)}$
07	Compute new fuzzy partition $u_{il}^{(t)},\ \forall i = 1\dots c$ and $\forall l \in \Omega^{(t)}$, using Eq. (18)
08	Compute new cluster prototypes $v_i^{(t)},\ \forall i = 1\dots c$, using Eq. (21)
09	Compute auxiliary lookup table values $q_l^{(t)},\ \forall l \in \Omega^{(t)}$, using Eq. (22)
10	Compute new estimated bias field $b_k^{(t)},\ \forall k = 1\dots n$, using Eq. (23)
11	Smoothen the estimated bias field using the chosen filter
12	Until convergence occurs, that is $\sum_{i=1}^{c} \lvert v_i^{(t)} - v_i^{(t-1)}\rvert < \varepsilon$
13	Assign pixel with index k ($k = 1\dots n$) to cluster with index $\underset{i}{\arg\max}\{u_{i,y_k - b_k},\ i = 1\dots c\}$

which can be further written

$$\sum_{l\in\Omega^{(t)}} h_l^{(t)} u_{il}^m l = v_i \sum_{l\in\Omega^{(t)}} h_l^{(t)} u_{il}^m. \tag{20}$$

Consequently, for any cluster indexed $i = 1\dots c$, we get the update formula:

$$v_i = \frac{\sum_{l\in\Omega^{(t)}} h_l^{(t)} u_{il}^m l}{\sum_{l\in\Omega^{(t)}} h_l^{(t)} u_{il}^m}. \tag{21}$$

This formula is evaluated c times in every iteration, like in case of conventional FCM-b, but here both the denominator and divisor of the fraction sum up much fewer terms.

Obviously the estimated bias field has to treat each pixel separately. But even here we can simplify the computations by introducing some auxiliary variables and organizing them into a lookup table. In this order, for any $l \in \Omega^{(t)}$, let

$$q_l = \frac{\sum_{i=1}^{c} u_{il}^m v_i}{\sum_{i=1}^{c} u_{il}^m}. \tag{22}$$

Subsequently, for any pixel with index $k = 1\dots n$, we have the bias estimated as:

$$b_k = y_k - q_{l_k} \quad \text{with} \quad l_k = y_k - b_k^{(t-1)}. \tag{23}$$

The AO scheme of the proposed objective function involves repeating the application of update formulas given in Eqs. (18), (21) and (23), until convergence is achieved. Pixels are assigned according to their compensated intensity $y_k - b_k$, towards the closest cluster prototype. The proposed compensation and segmentation algorithm is summarized in Table 2.

4. Results and discussions

Looking at the formulas used by the conventional and accelerated approach, we can realize the difference in theoretical complexity of different steps. These theoretical values are

Table 3 – Computational complexity of algorithmic steps.

Algorithmic step	Conventional (FCM-b)	Accelerated (FCM-qb)
Partition updating	$\mathcal{O}(nc^2)$	$\mathcal{O}(\omega c^2)$
Cluster prototype updating	$\mathcal{O}(nc)$	$\mathcal{O}(\omega c)$
Bias estimation	$\mathcal{O}(nc)$	$\mathcal{O}(n+\omega c)$
Bias smoothing	$\mathcal{O}(n)$	$\mathcal{O}(n)$
Histogram updating	–	$\mathcal{O}(n)$

exhibited in Table 3, where ω stands for the cardinality of the set Ω or the number of different intensity values in the current compensated image. Considering the fact that the number of present gray intensities (ω) is less than the number of pixels (n) in the image by minimum two orders of magnitude, we can state that the time consuming first three steps of the conventional algorithm are replaced with much faster solutions in the proposed algorithm.

Both the conventional and proposed approaches were tested on artificial phantoms and real MR images. Artificial phantoms were created by adding slowly varying INU noise to single-channel intensity images that contained two easily separable regions of constant intensity. Real MR images were taken from the Internet Brain Segmentation Repository [8]. All benchmark results were obtained on a PC with Athlon64 processor running at 2 GHz frequency.

Fig. 1 summarizes the averaged benchmark results of both algorithms, obtained from 24 different artificial phantoms, sampled at various resolutions. In case of two classes, the proposed formulation of the algorithm accelerates the execution about 15–25 times. It is also visible, that the speed-up ratio slightly rises if we increase the size of the input phantom image.

Fig. 2 shows the variation of the histogram of a phantom image during the iterative compensation. The two classes are perfectly separated after 10–12 iteration cycles. The regions

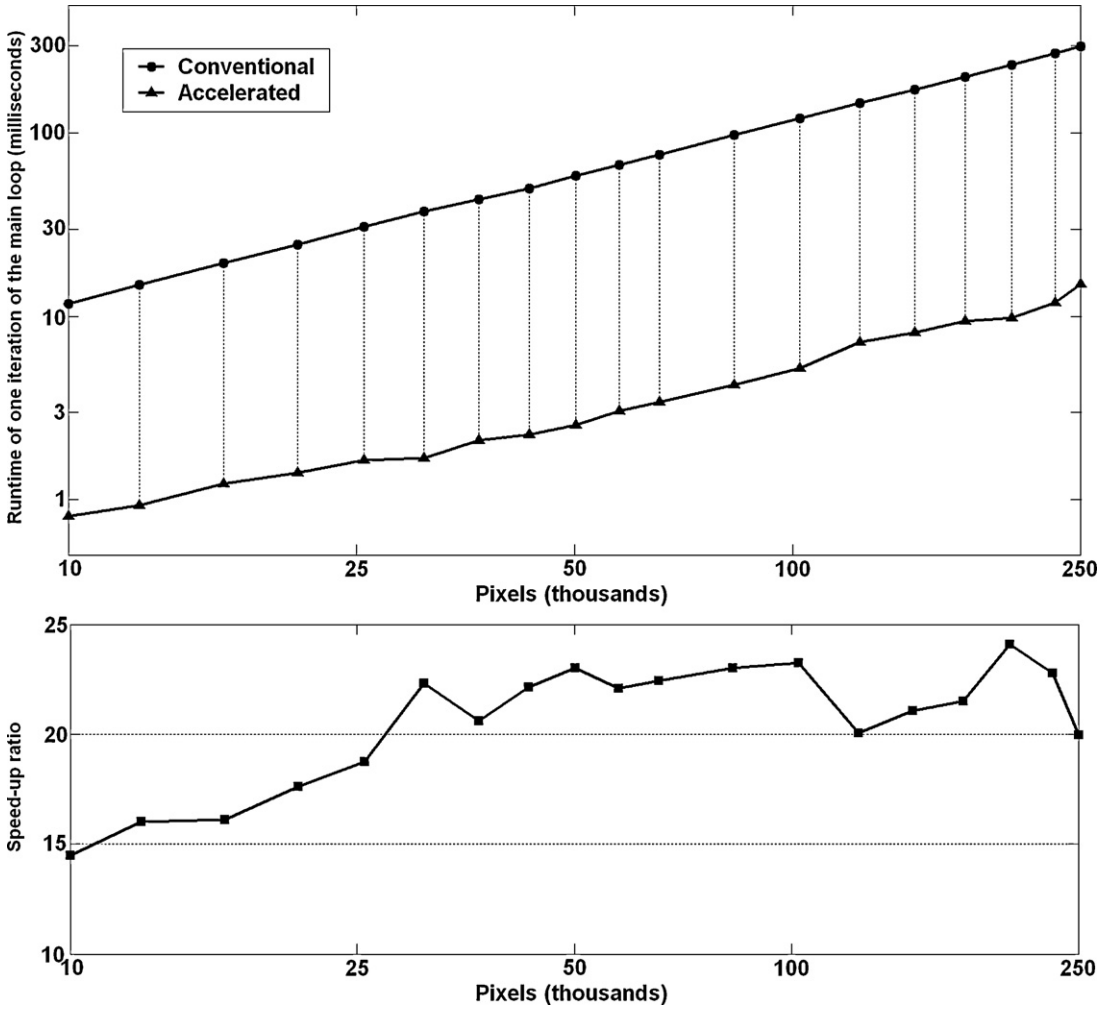

Fig. 1 – Execution time of one main loop, using the conventional and accelerated approach (up), and the resulting speed-up ratio (down), all represented against the number of pixels in the image (n). These benchmark results were recorded using phantom images, segmented into $c = 2$ classes.

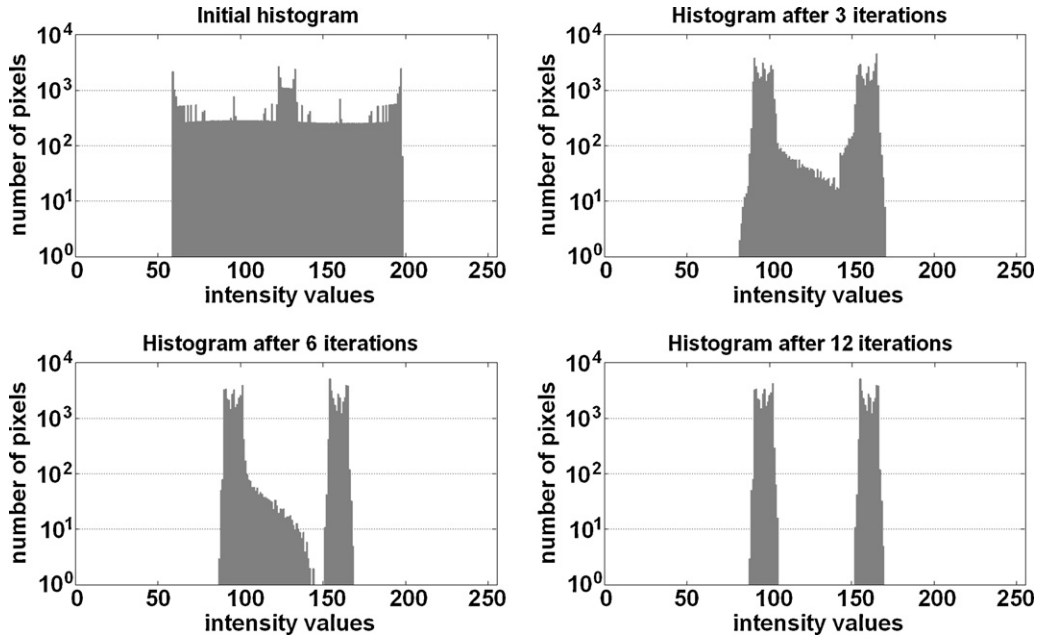

Fig. 2 – The evolution of the histogram of an INU contaminated two-class phantom image, during the iteration cycles.

the compensation produces are not piecewise constant, but they are easily separable, so the classification can be 100% accurate.

Fig. 3 exhibits the segmentation and INU compensation of a two-class phantom. Without compensation the segmentation fails, but compensation makes the classes perfectly separable.

Real brain MR images of different sizes, artificially contaminated with inhomogeneity were also fed to both algorithms. These images were segmented into $c = 3$ classes corresponding to white matter (WM), gray matter (GM), and cerebro-spinal fluid (CSF), respectively. Benchmark results averaged from the outcome of the algorithm using 40 different real MR images are exhibited in Fig. 4. The speed-up ratio is even higher than in case of the phantoms: it varies between 28 and 32.

Fig. 5(a)–(e) shows the variation of the histogram of a brain MRI image segmented into three clusters, during the iterative compensation. In this latter case, convergence requires 60–100 iterations. As the white matter and gray matter have their intensities close to each other, in the presence of noise, their histograms overlap, so their distributions cannot be completely separated by INU compensation. This is a primary source of misclassifications, equally present for both the conventional and proposed approaches. The evolution of the three cluster prototypes exhibited in Fig. 5(f) represents a typical case of real MRI image segmentation which converges after 60 iterations. Fig. 6 exhibits the intermediary and final results of the segmentation of a real MR brain image.

As $c \ll \omega \ll n$, the theoretical complexity values exhibited in Table 3 suggest that the running time of the accelerated algorithm hardly depends on the number of clusters. To confirm this hypothesis, we have fed various images to the algorithm, setting the number of clusters c to values ranging from 2 to 8. Fig. 7 summarizes the speed-up ratios, their averaged values using 25 images, and their standard deviations as well. This plot indicates that as we increase the number of clusters at the segmentation of an image, the obtained speed-up ratios keep rising indeed.

Fig. 8 shows the relative execution times of different steps within one iteration of both approaches. The acceleration is also evident in this figure: INU smoothing consists of the same

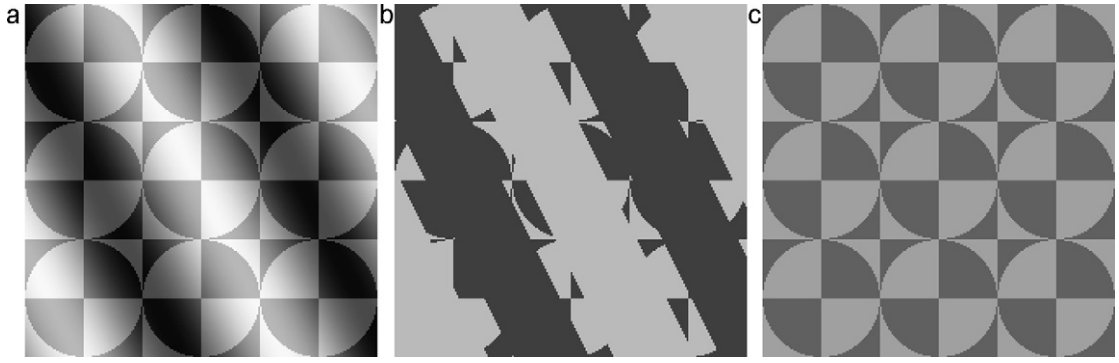

Fig. 3 – Phantom segmentation into two classes: (a) original image, (b) failed segmentation without INU compensation, and (c) successful segmentation with INU compensation.

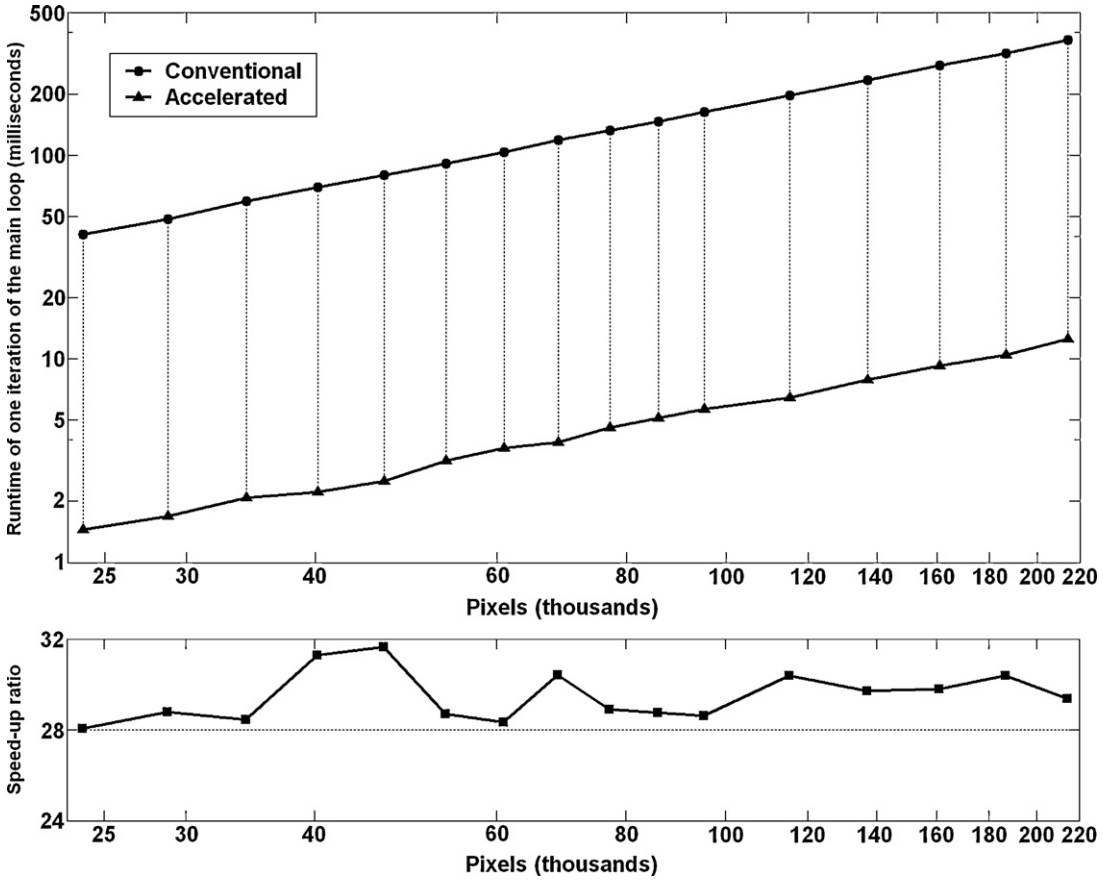

Fig. 4 – Execution time of one main loop, using the conventional and accelerated approach (up), and the resulting speed-up ratio (down), all represented against the number of pixels in the image. These benchmark results were recorded using phantom images, segmented into c = 3 classes.

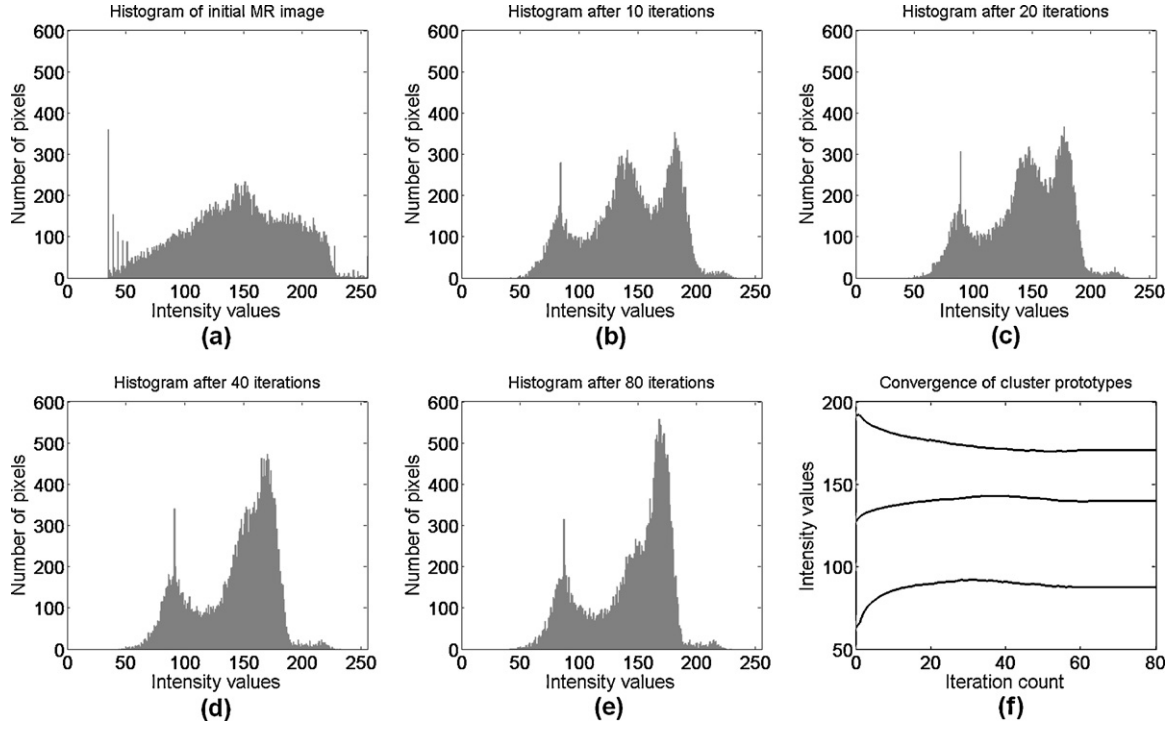

Fig. 5 – (a)–(e) The evolution of the intensity distribution of an INU contaminated real MR image during the iteration cycles and (f) the evolution of cluster prototypes during the iterations.

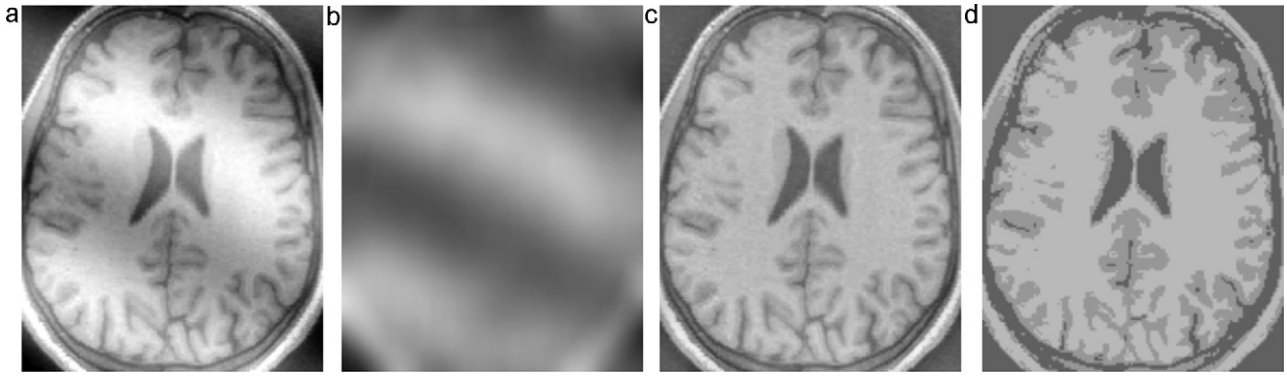

Fig. 6 – Brain segmentation into three classes: (a) original image, (b) estimated INU, (c) compensated image, and (d) successful segmentation with INU compensation.

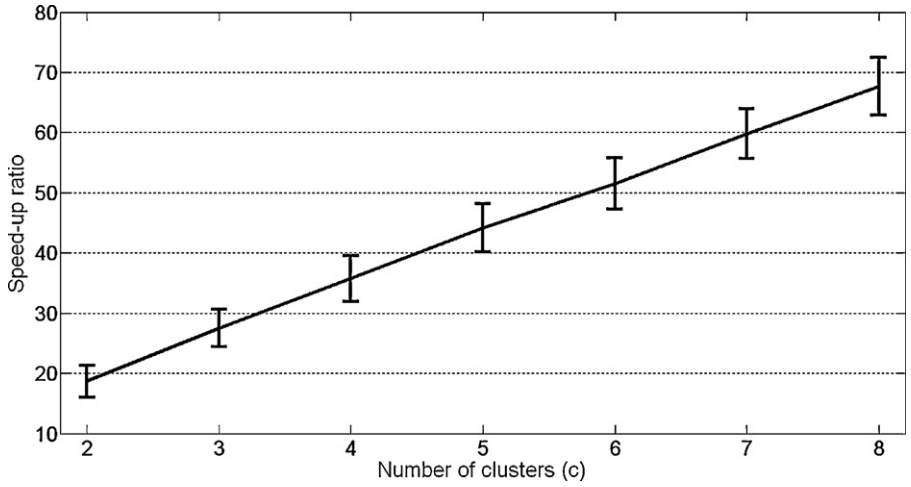

Fig. 7 – Average and standard deviation of the obtained speed-up ratios, plotted against cluster count.

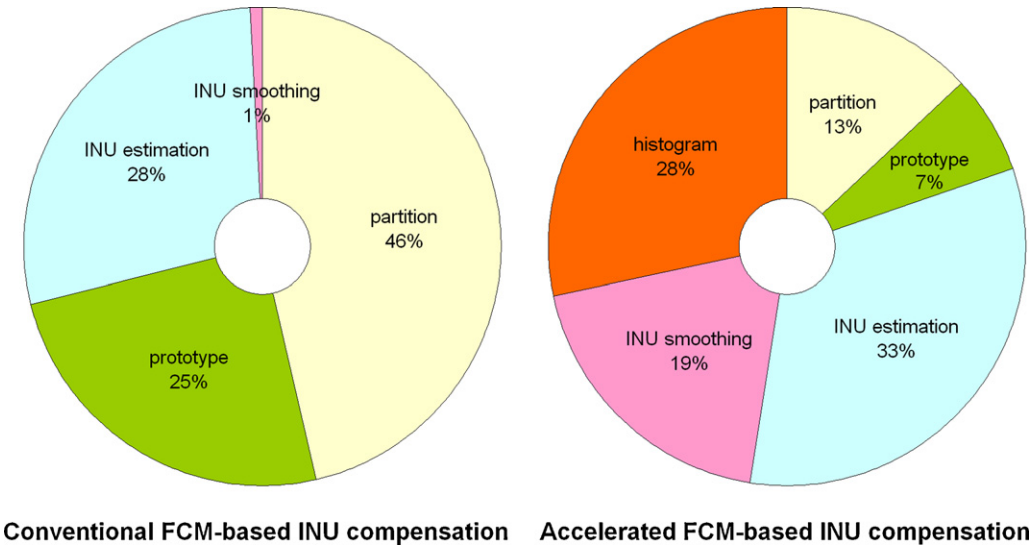

Fig. 8 – Structure of the runtime in both approaches.

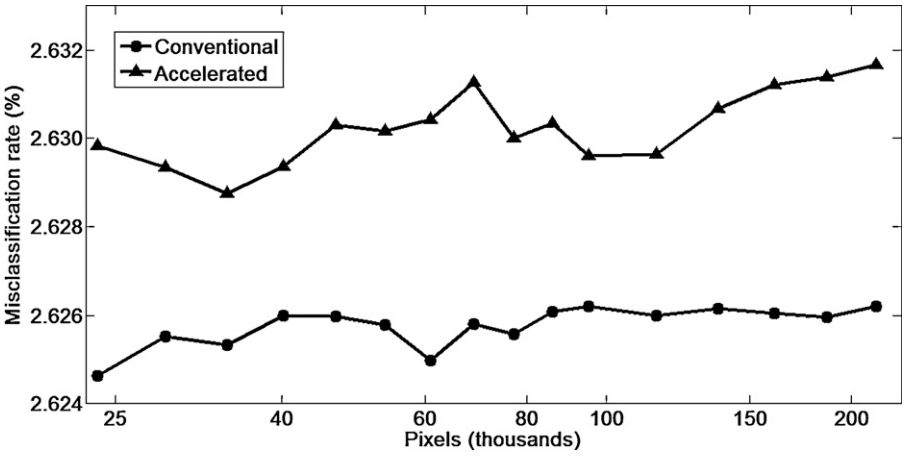

Fig. 9 – Evolution of the misclassification rate vs. image size in case of a typical case of real MRI.

operations in both approaches, but it takes less then 1% in the conventional approach and 19% in the proposed algorithm. In the conventional approach, partition updating represents the highest computational load, while in the proposed approach, the locally executed INU estimation and the newly introduced histogram updating step are the longest processes.

Both approaches theoretically perform the same computations, so the accelerated approach should have exactly the same accuracy as the conventional one. However, in practice, there is a secondary source of errors in the proposed approach due to the quantification error of the bias field. The conventional algorithm may employ floating point representation of the estimated bias field, while the proposed fast approach has to quantify the bias in every iteration. During the performed tests, bias quantification caused no more than 1% increase the number of misclassifications. Fig. 9 shows the slight effect of the bias quantification upon the count of misclassified pixels.

Further advantages of the proposed approach include:

- It is compatible with most INU modeling schemes enumerated in Section 2.2. Also in case of modeling INU as log-bias field, the partition and cluster prototypes can be computed using the histogram, just as we have shown in the bias field formulation. However, in case of the gain field approach, the cluster prototype update formula will include local factors. In this latter case, a lower speed-up ratio of 5–10 can be achieved.
- The proposed method is insensitive to the chosen bias smoothing procedure: the user has the freedom to apply reported techniques like the mean spread filtering [16], or the morphological criterion driven context dependent filtering [20].
- The proposed method is not limited to fuzzy *c*-means clustering. It can be similarly applied with mixed clustering models presented in [12,21,22].

5. Conclusion

In this paper, we have reformulated the *c*-means clustering based approach of INU compensation and segmentation of magnetic resonance images, in order to drastically reduce the processing time. We have shown that the most time consuming parts of the conventional algorithm's iteration cycle can be applied to individual gray intensities instead of individual pixels. We achieved an approach that performs the segmentation of brain MR images 20–30 times faster, without causing relevant change in terms of accuracy. The proposed algorithm is highly compatible with various reported *c*-means clustering based INU compensation techniques. With this increased execution speed, the *c*-means clustering approach may receive a significantly higher popularity in the domain of MR image segmentation.

Conflict of interest

None declared.

Acknowledgements

The work of L. Szilágyi and S. M. Szilágyi was supported by János Bolyai Fellowship Program of the Hungarian Academy of Sciences. The work of B. Benyó was supported by the New Széchenyi Plan (Project ID: TÁMOP-4.2.1/B-09/1/KMR-2010-0002), and the Hungarian National Scientific Research Foundation, Grant Nos. T80316 and T82066.

REFERENCES

[1] M.N. Ahmed, S.M. Yamany, N. Mohamed, A.A. Farag, T. Moriarty, A modified fuzzy *c*-means algorithm for bias field estimation and segmentation of MRI data, IEEE Transactions on Medical Imaging 21 (3) (2002) 193–199.
[2] L. Axel, J. Costanini, J. Listerud, Inhomogeneity correction in surface-coil MR imaging, American Journal of Roentgenology 148 (2) (1987) 418–420.
[3] J.C. Bezdek, Pattern Recognition with Fuzzy Objective Function Algorithms, Plenum, New York, NY, 1981.
[4] J.C. Bezdek, L.O. Hall, L.P. Clarke, Review of MR image segmentation techniques using pattern recognition, Medical Physics 20 (4) (1993) 1033–1048.

[5] B.H. Brinkmann, A. Manduca, R.A. Robb, Optimized homomorphic unsharp masking for MR grayscale inhomogeneity correction, IEEE Transactions on Medical Imaging 17 (2) (1998) 161–171.
[6] W. Cai, S. Chen, D.Q. Zhang, Fast and robust fuzzy c-means algorithms incorporating local information for image segmentation, Pattern Recognition 40 (3) (2007) 825–838.
[7] J. Derganc, B. Likar, F. Pernuš, Nonparametric segmentation of multispectral MR images incorporating spatial and intensity information, in: Proceedings of SPIE Medical Imaging, vol. 4684, 2002, pp. 391–400.
[8] Internet Brain Segmentation Repository. Available at: http://www.cma.mgh.harvard.edu/ibsr.
[9] B. Johnston, M.S. Atkins, B. Mackiewich, M. Anderson, Segmentation of multiple sclerosis lesions in intensity corrected multispectral MRI, IEEE Transactions on Medical Imaging 15 (2) (1996) 154–169.
[10] R. Krishnapuram, J.M. Keller, A possibilistic approach to clustering, IEEE Transactions on Fuzzy Systems 1 (2) (1993) 98–110.
[11] A.W.C. Liew, Y. Hong, An adaptive spatial fuzzy clustering algorithm for 3-D MR image segmentation, IEEE Transactions on Medical Imaging 22 (9) (2003) 1063–1075.
[12] N.R. Pal, K. Pal, J.M. Keller, J.C. Bezdek, A possibilistic fuzzy c-means clustering algorithms, IEEE Transactions on Fuzzy Systems 13 (4) (2005) 517–530.
[13] D.L. Pham, J.L. Prince, Adaptive fuzzy segmentation of magnetic resonance images, IEEE Transactions on Medical Imaging 18 (9) (1999) 737–752.
[14] J.C. Rajapakse, J.C. Kruggel, Segmentation of MR images with intensity inhomogeneities, Image and Vision Computing 16 (3) (1998) 165–180.
[15] A. Simmons, P.S. Tofts, G.J. Barker, S.R. Arrdige, Sources of intensity nonuniformity in spin echo images at 1.5 T, Magnetic Resonance in Medicine 32 (1) (1994) 121–128.
[16] M.Y. Siyal, L. Yu, An intelligent modified fuzzy c-means based algorithm for bias field estimation and segmentation of brain MRI, Pattern Recognition Letters 26 (13) (2005) 2052–2062.
[17] J.G. Sled, A.P. Zijdenbos, A.C. Evans, A nonparamtertic method for automatic correction of intensity nonuniformities, IEEE Transactions on Medical Imaging 17 (1) (1998) 87–97.
[18] M. Styner, C. Brechbuchler, G. Székely, G. Gerig, Parametric estimate of intensity inhomogeneities applied to MRI, IEEE Transactions on Medical Imaging 19 (3) (2000) 153–165.
[19] L. Szilágyi, Z. Benyó, S.M. Szilágyi, H.S. Adam, MR brain image segmentation using an enhanced fuzzy c-means algorithm, in: Proceedings of the 25th Annual International Conference of IEEE EMBS, 2003, pp. 724–726.
[20] L. Szilágyi, S.M. Szilágyi, Z. Benyó, Multi-stage FCM-based intensity inhomogeneity correction for MR brain image segmentation, Lecture Notes in Computer Science 5164 (2008) 527–536.
[21] L. Szilágyi, S.M. Szilágyi, B. Benyó, Z. Benyó, Intensity inhomogeneity compensation and segmentation of MR brain images using hybrid c-means clustering models, Biomedical Signal Processing and Control 6 (1) (2011) 3–12.
[22] L. Szilágyi, Fuzzy-possibilistic product partition: a novel robust approach to c-means clustering, Lecture Notes in Computer Science 6820 (2011) 150–161.
[23] P. Vemuri, E.G. Kholmovski, D.L. Parker, B.E. Chapman, Coil sensitivity estimation for optimal SNR reconstruction and intensity inhomogeneity correction in phased array MR imaging, Lecture Notes in Computer Science 3565 (2005) 603–614.
[24] E.A. Vokurka, N.A. Watson, Y. Watson, N.A. Thacker, A. Jackson, Improved high resolution MR imaging for surface coils using automated intensity non-uniformity correction: feasibility study in the orbit, Journal of Magnetic Resonance Imaging 14 (5) (2001) 540–546.
[25] U. Vovk, F. Pernuš, B. Likar, MRI intensity inhomogeneity correction by combining intensity and spatial information, Physics in Medicine and Biology 49 (17) (2004) 4119–4133.
[26] U. Vovk, F. Pernuš, B. Likar, A review of methods for correction of intensity inhomogeneity in MRI, IEEE Transactions on Medical Imaging 26 (3) (2007) 405–421.
[27] Y. Zhang, M. Brady, S.S. Smith, Segmentation of brain MR images through a hidden Markov random field model and the expectation-maximization algorithm, IEEE Transactions on Medical Imaging 20 (1) (2001) 45–57.